Determining the parameters governing the electrochemical stability of thiols and disulfides self-assembled monolayer on gold electrodes in physiological medium

Kolodziej, Adam; Fernandez-Trillo, Francisco; Rodriguez, Paramaconi

DOI:
10.1016/j.jelechem.2017.07.039

Document Version
Peer reviewed version

Citation for published version (Harvard):
Kolodziej, A, Fernandez-Trillo, F & Rodriguez, P 2017, 'Determining the parameters governing the electrochemical stability of thiols and disulfides self-assembled monolayer on gold electrodes in physiological medium', Journal of Electroanalytical Chemistry. https://doi.org/10.1016/j.jelechem.2017.07.039

Determining the parameters governing the electrochemical stability of thiols and disulfides self-assembled monolayer on gold electrodes in physiological medium

Adam Kolodziej,[1] Francisco Fernandez-Trillo[1,2,3,*] Paramaconi Rodriguez[1,*]

[1]School of Chemistry, [2]School of Pharmacy, and [3]Institute of Microbiology and Infection, University of Birmingham, Edgbaston, B15 2TT, UK

*corresponding authors: f.fernandez-trillo@bham.ac.uk , p.b.rodriguez@bham.ac.uk

Abstract

Herein we study the electrochemical potential-dependent and time-dependent stability representative of thiols and disulfides as self-assembled monolayers on gold electrodes. The stability of four representative sulfur-containing compounds: 3-mercaptopropionic acid , 2-mercaptoethanol , 1,4-dithiothreitol and DL-thioctic acid , was assessed in simulated physiological conditions (i.e. phosphate buffer saline). The stability of these molecules was evaluated using cyclic voltammetry and step-potential chronoamperometry. Coordination of the thiols and disulfides significantly affects the stability of the self-assembled monolayer. In addition, studies performed using gold single crystal (100) and (111) electrodes show the superior binding strength of the SAM on the Au(100) surface structure.

Graphical abstract

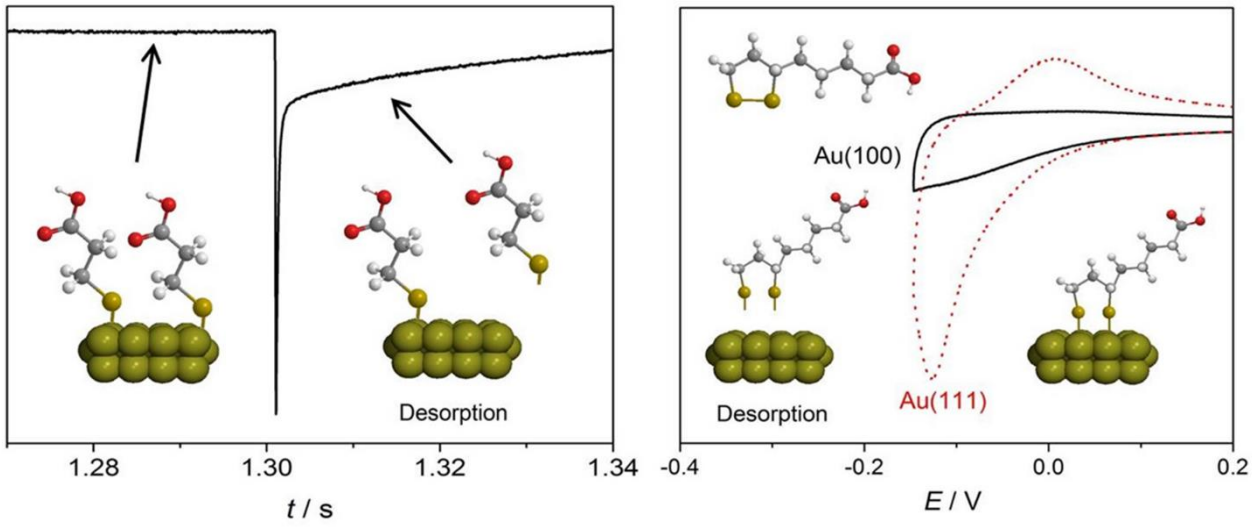

Keywords: self-assembly monolayer of thiols, disulfides, electrochemistry, desorption, surface structure

1. Introduction

The functionalization of metal surfaces by self-assembled monolayers (SAMs) of alkanethiols and closely related compounds is a continuously expanding area with enormous impact on corrosion, lubrication, biomimetics, and sensing among others fields.[1-7] Recently, SAMs have also found relevant applications in drug/gene delivery and imaging.[8, 9] The controlled release of drugs and related compounds, is highly relevant in medical applications, for instance to minimize negative side effects, as well as extend the circulation and half-life of these bioactive compounds.[1, 10-12] Thiol-functionalized molecules have been widely studied by electrochemical means due to its importance in mentioned areas. Understanding the stability of these S-Au SAMs is of paramount importance to benchmark the reliability and reproducibility of the electrochemical devices fabricated with these materials.[13-15] For example, in the development of electrochemical sensors, a robust and stable monolayer would be desirable, in particular one that can operate in a wide potential window. However, SAMs are subject to oxidative and reductive desorption that

compromises the integrity of the monolayer. Reductive desorption is more restrictive due to its occurrence at the potentials more likely to be analytically useful. [16,17] For these reasons, reductive desorption of thiols from gold surfaces have been studied by a variety of electrochemical, probe microscopy and spectroelectrochemical techniques.[13-15, 18-34]. While electrochemical and spectroelectrochemical methods provide important information on the coverage, potential window stability and the charge number per molecule adsorbed; in situ probe microscopy gives information about the packing, unit cell and adsorption symmetry of thiols as a function of the potential. Previous studies have been mostly conducted using cyclic voltammetry (CV) and chronoamperometry (CA) in alkaline media due to the high solubility of thiolates under these conditions. Important contributions to the understanding on thiols coverage and stability on model systems have been reported by Lipkowski group over the last two decades. Recently, Kunze et al. and Laredo et at. have reported the importance of the methodology implemented to determine the coverage of thiol monolayers on Au(111) single crystal electrodes. In these reports it is highlighted how reductive desorption methods present systematic errors due to the uncertainities associated with the charging current correction. These authors introduced a step potential chronocoulometry as a potentiostatic method to measure the charge density at the electrode at different potentials in 0.1 M NaF, 0.1M $HClO_4$ and 0.1 M NaOH.[13-15] However, the understanding of the stability of adsorbed sulfur-containing molecules on gold electrodes at physiological conditions has enormous implications in sensing and the controlled delivery of drugs in blood (pH=7.2-7.6).[35-37] Noteworthy, in addition to the pH, the reductive desorption of thiols is influenced by the surface structure of the metal substrate. Such structure-reactivity relationship is attributed to the different coordination of surface atoms[19] and a difference in binding energies to various basal planes.[21, 22, 28, 38-40] In order to provide a rational understanding of the role of the surface structure on the stability of thiols in electrochemical media, spectroelectrochemical methods have been also used.[18, 29, 30] Recently, Bizzotto et al. have used fluorescence microscopy and thiols tagged with fluorescent probes to track the reductive desorption of thiols as a function of the surface structure of

polyoriented bead-type gold electrodes.[18, 31] The report by Bizzotto concludes that (111) is more amenable to desorption of thiol SAMs when compared to the other surface sites of the polycrystalline gold electrode.

The implementation of thiols SAM in controlled delivery of drugs and nanosensing requires an understanding of the parameters governing the desorption of thiols from polycrystalline surfaces that mimic monocrystalline surfaces and its behaviour in physiological media.

Aware of these needs, here we present a progressive step-potential approach that provides potential and time-dependence insights of the reductive desorption of adsorbed monolayers of thiols from polycrystalline gold electrodes in a physiological media containing phosphate and chloride ions. The protocol was evaluated over 4 representative sulfur-containing molecules: 3-mercaptopropionic acid (**1**), 2-mercaptoethanol (**2**), 1,4-dithiothreitol (**3**) and DL-thioctic acid (**4**) in a phosphate saline buffer solution (DPBS). The progressive step-potential experiments provide relevant information on the stability of the thiols as a function of their nature; at the same time these experiments provide relevant information on the kinetics of the reductive desorption process. We also evaluated the influence of the surface structure of the gold electrode for the desorption of two selected compounds: 3-mercaptopropionic acid (**1**) and DL-thioctic acid (**4**) in a phosphate saline buffer solution.

2. Experimental

An exhaustive cleaning procedure of the glassware was implemented to ensure reproducible experimental conditions.[41] On a daily basis, the glassware was soaked overnight in an acidic solution of $KMnO_4$. The glassware was then removed from the $KMnO_4$ solution, and rinsed with a diluted solution of H_2SO_4/H_2O_2 with a ratio of 1:3. The glassware was finally rinsed with boiling Milli-Q water (18.2 MΩ cm, 1 ppb total organic carbon) at least 5 times to ensure the absence of sulfate ions in the working solution. A three compartment electrochemical cell was employed with a high surface area gold flag counter electrode and a Hg/Hg_2SO_4 reference electrode. All the results were converted to RHE scale as presented in the manuscript. Measurements were performed on

μAutoLab III potentiostat. Prior to experiments, Argon (6N, BOC) was used to deoxygenate electrolytic media.

Gold disk electrodes were prepared from high purity (Sigma Aldrich, 99.999%) gold wire. Prior to each experiment, the gold disk electrode was mechanically polished with diamond slurry, rinsed with Milli-Q water, flame-annealed and cooled down under argon atmosphere.

Au(111) and Au(100) bead-type single-crystal electrodes (icryst) were flame annealed and cooled down in Ar atmosphere prior to each experiment. The blank voltammetry of the gold electrode was registered prior to each set of experiments to confirm the cleanness of the system (both electrode and electrolyte). Dulbecco's Phosphate Buffer Saline solution (DPBS pH= 7.4, Lonza) was used as the electrolyte throughout the manuscript. This electrolyte was selected to mimic physiological conditions (i.e. pH and osmolarity) and has been used in a range of scientific reports including examples in drug delivery[42] or cells culture[43]. All the experiments were performed at room temperature which fluctuates between 14°C and 20°C.

Gold electrodes were functionalised with self-assembled layers of the desired compound by immersing the clean gold electrode, following flame-annealing and rinsing with Milli-Q water, in a solution containing 10 mM of the desired compound. The gold electrode was immersed for 10 min at open circuit potential (OCP). Solutions were prepared as follows: 3-mercaptopropionic acid (**1**) (Sigma Aldrich, ≥ 99%) in 3:1 mixture of Milli-Q water and absolute ethanol; 2-mercaptoethanol (**2**) (Sigma Aldrich, ≥ 99%) and 1,4-dithiothreitol (**3**) (Sigma Aldrich, ≥ 98%) in Milli-Q water; and DL-thioctic acid (**4**) (Alfa Aesar, 98%) in absolute ethanol. The excess of physisorbed molecules was removed by rinsing with a copious amount of Milli-Q water.

3. Results and discussion

3.1 Assessment of the stability of 3-mercaptopropionic acid, 2-mercaptoethanol, 1,4-dithiothreitol and DL-thioctic acid on Au polycrystalline electrode in phosphate buffer solution.

Figure 1 shows the voltammetric profiles of the surface-modified Au electrodes with the four different compounds evaluated **1**-**4**. The blank voltammetry of bare gold polycrystalline electrode is included for comparison. In all the cases, a decrease of the double-layer charging current can be observed while the features associated to the lifting of the reconstruction of Au and to the adsorption/desorption of phosphate anions disappear.[44] These changes in the voltammetric profile are a clear evidence of the presence of compounds **1**-**4** on the surface. Differences in the capacitive current for each molecule correspond to different surface defects formed by each monolayer.[45]

In these voltammetric profiles, several features could be identified. At lower potentials (-0.15 to 0.25 V vs RHE) reduction peaks associated to the irreversible desorption of the compounds were observed.[23] The onset potential for the reductive desorption of monothiols (**1**) and (**2**), appeared at more positive values than those for the reductive desorption of compounds (**3**) and (**4**), which showed similar desorption kinetics. This difference in potential is associated to the higher stability of those compounds containing two sulfur atoms with respect to the monothiols.[16]

When we compared both monothiols, the desorption of 3-mercaptopropionic acid (**1**) was much faster than the desorption of 2-mercaptoethanol (**2**). We believe that the bulky carboxylic group in (**1**) may affect the order of the monolayer, resulting in a higher number of defects, or pinholes, in the adlayer. The presence of pinholes results in the desorption of thiols,[26] a process that thus happens at more positive potentials.[46, 47] This is in agreement with the larger double layer capacity observed in the case of **(1)**, as a consequence of a lower surface coverage.[45] Previous results have also shown that the interaction between the hydroxyl groups of 2-mercaptoethanol (**2**) might play a significant role in the adsorption step of 2-mercaptoethanol on Au(111) resulting in different commensurable and incommensurable structures. The presence of multiple overlapping signals on

the desorption of both monothiols (**1**) and (**2**) can be associated to the desorption from different surface structures, the stability of the different incommensurable and commensurable phases of the thiols, or the combination of both (see discussion below).

Finally, from voltammetric profiles we could conclude that the desorption of the thiols was not reversible, as evidenced by the lower charge on the anodic process observed during the positive scan.

Due to the uncertainties associated to the double layer charging correction and the reconstruction of the gold surface, in particular for polycrystalline electrodes, determining the charge for the desorption of thiols from a cyclic voltammetry results in a large error.

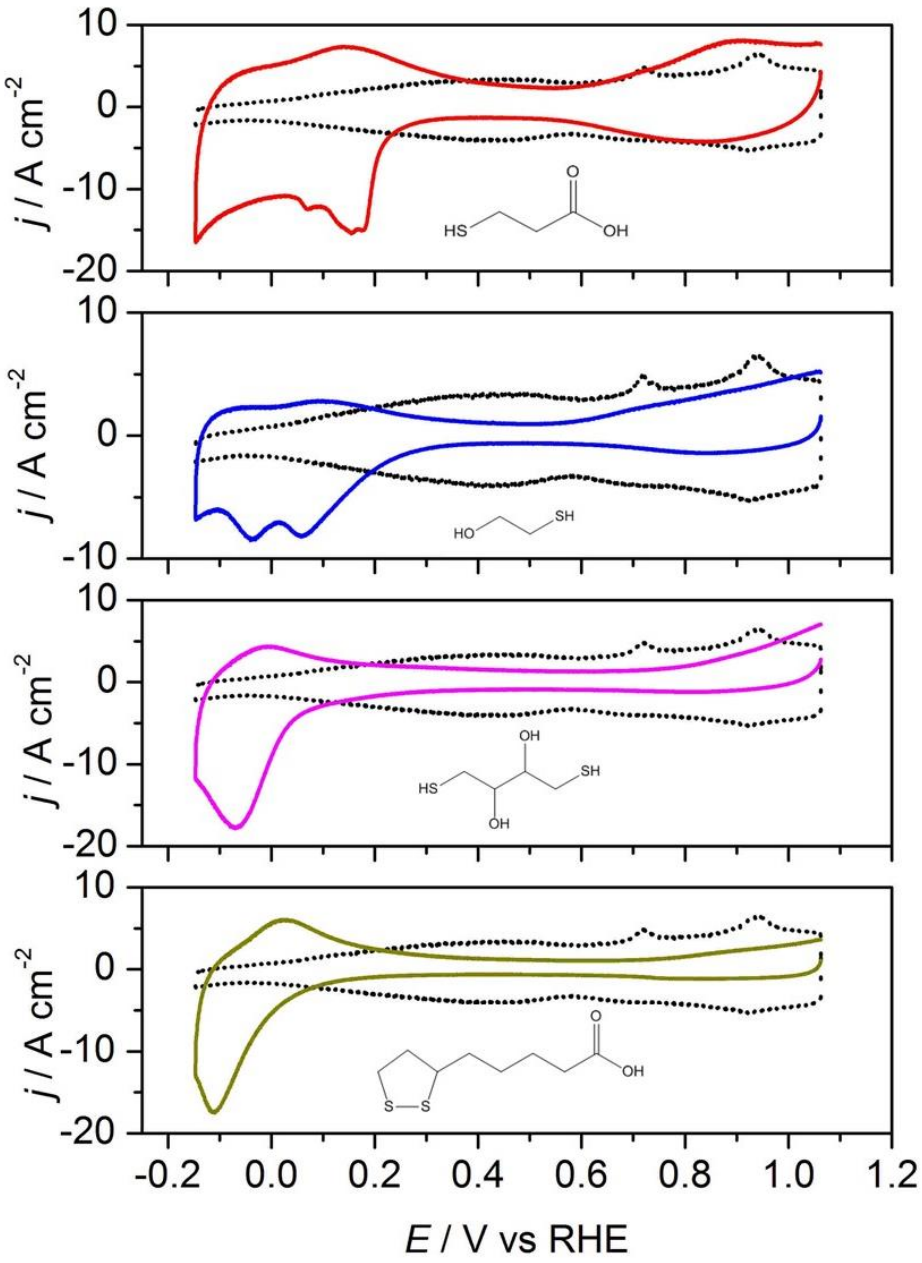

Figure 1. Voltammetric profiles of polycrystalline gold electrodes modified with 3-mercaptopropionic acid (1), 2-mercaptoethanol (2), 1,4-dithiothreitol (3) and DL-thioctic acid (4) recorded in DPBS. Blank voltammetries of the electrodes in absence of the adsorbed molecules are shown for comparison (dotted line). Scan rate υ = 50 mV s^{-1}.

In order to gain quantitative insights on the stability and desorption kinetics of these sulfur containing molecules from the gold surfaces, a chronoamperometric method was developed (Figure 2A). Previous work by Lipkowski group[13-15] developed and implemented a chronoamperometric method to determine the charge of adsorbed molecules and packing densities of self-assembled

monolayers of long chain aliphatic thiols and on single crystal electrodes. Due to the differences in the nature and structure of the molecules (long chain aliphatic thiols vs short chain thiols and disulfides), and the differences of the surface structure of the gold electrodes (single crystal vs polycrystalline electrodes) the implementation of this protocol and the determination of the packing of the molecules was not possible. As an alternative, we have modified the protocol: a progressive step-potential strategy was implemented to supress large contributions associated to the charging of the double layer on the current transients. The protocol relies on the application of 10 successive potentials steps (0.05 s each) where only one of the steps is prolonged up to 1 s. This prolonged step provides a distinctive signal of the desorption of the molecules at the given potential. The protocol was applied to 5 desorption potentials: 0.25, 0.15, 0.05, -0.05 and -0.15 V vs RHE ; for sake of clarity only the results for desorption potentials between 0.15 and -0.15 V vs RHE are shown.

Figure 2B shows the polarization curves for the progressive step-potential protocol on the 2-mercaptoethanol-modified gold electrode. The polarization curves of the progressive step-potential experiments of (**1**), (**3**) and (**4**) are shown on figure S1.

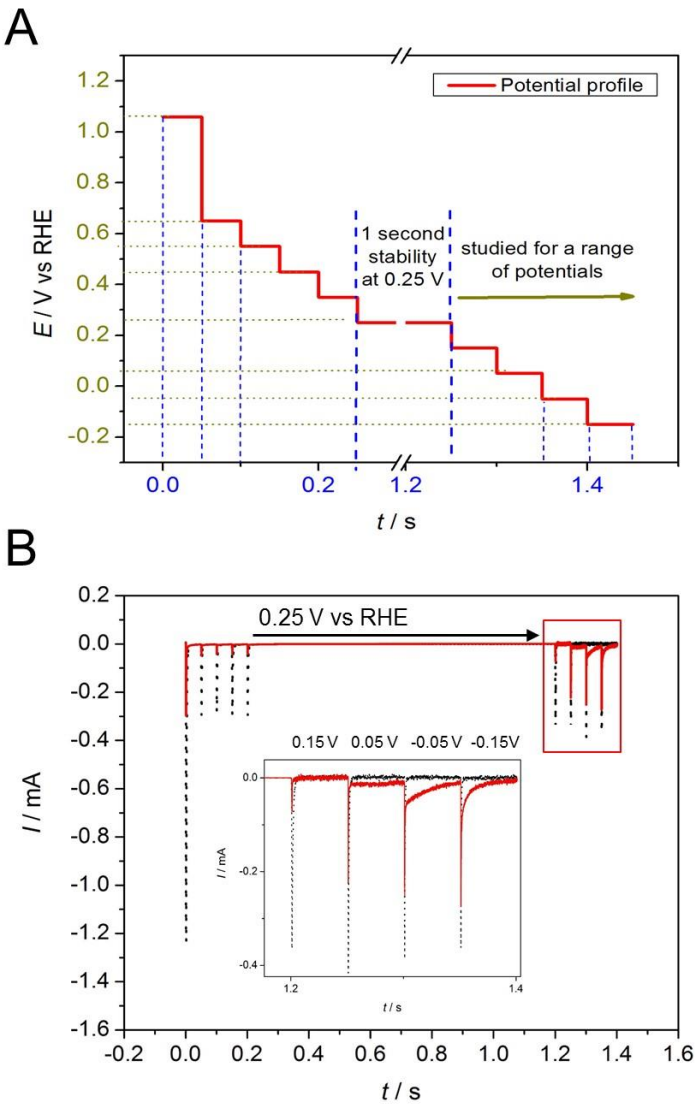

Figure 2. (A) Representative experimental procedure for the progressive potential-step chronoamperometry for which each potential step is probed for 0.05 s except one that is probed for 1s (0.25 V vs RHE in the example shown). This prolonged treatment is systematically applied at each potential step. (B) Progressive potential-step chronoamperometry recorded for a bare polycrystalline gold electrode (black dotted line) and for a polycrystalline gold electrode modified with 3-mercaptopropionic acid (1) (red solid line) with 1 s step at 0.25 V vs RHE. Inset shows a close up of the desorption at potentials lower than 0.25 V vs RHE.

As can be seen in the inset of figure 2, the sharp current transient at each potential step associated to the fast double layer charging is followed by smooth current transient which we assign to the slow desorption of the chemisorbed molecules at the given potential. The selection of the time scale of

the steps, guarantee the total desorption of the molecule at the given potential, as the current decreases to zero before the next potential is applied. When the modified electrode was probed for a shorter period of time (≤ 0.5s) (Figure S2), the partial desorption of the thiols due to the slow kinetics of desorption affected the quantitative analysis.

Quantitative information on the desorption process of these molecules as a function of the potential was obtained by integrating the charge under each step potential. An example of the potential limits and baseline taken for the integration are shown in Figure S3. The resulting values of the integrated charge as a function of applied potential, -0.05 and -0.15 V, are shown in the Figure 3.The comparison of the desorption charges for the potentials between 0.25 and -0.15V are presented in Figure S4.

The step potential experiments confirm the low stability of the monothiols (**1)** and (**2)** in comparison with the stability of (**3**) and (**4**) adsorbed on gold. The desorption of each of the compounds was potential dependent and only a partial desorption of the compounds took place at every single potential. The onset potential for desorption of (**1**) and (**2**) appeared at 0.1 V vs RHE in both cases. The onset potential determined using step-potential chronoamperometries is slightly less positive to the onset potential estimated from cyclic voltammetries (0.2 V vs RHE). This is related to the uncertainty of the value of the cyclic voltammetry due to the overlapping of the desorption process of the thiol and the adsorption/desorption of anions. The desorption process of the thiol was favoured when a longer step potential of 1s was applied at -0.05 V and -0.15 V. However, additional charge, but of lower magnitude, was measured at more negative potentials indicating the need for a more negative potential to trigger the desorption of the remaining strongly adsorbed molecules. This trend can be associated to the formation of different phases at the different surface sites present on the polycrystalline electrode. It is expected that the surface is dominated by (111) adsorption sites while (100) adsorption sites and step sites appear in smaller proportions. As it will be discussed in the second part of this manuscript, the desorption of these compounds is favoured at early potentials on the (111) surface structure.

The onset potential for desorption of the molecules containing two sulfur atoms (**3**) and (**4**) appeared at more negative potentials (-0.05 V vs RHE), suggesting a stronger interaction between these molecules and the gold surface. In both cases, the charge associated to the desorption process increased at more negative potentials and just in the case 1,4-dithiothreitol (**3**), the charge associated to the desorption slightly decreased at -0.15 V.

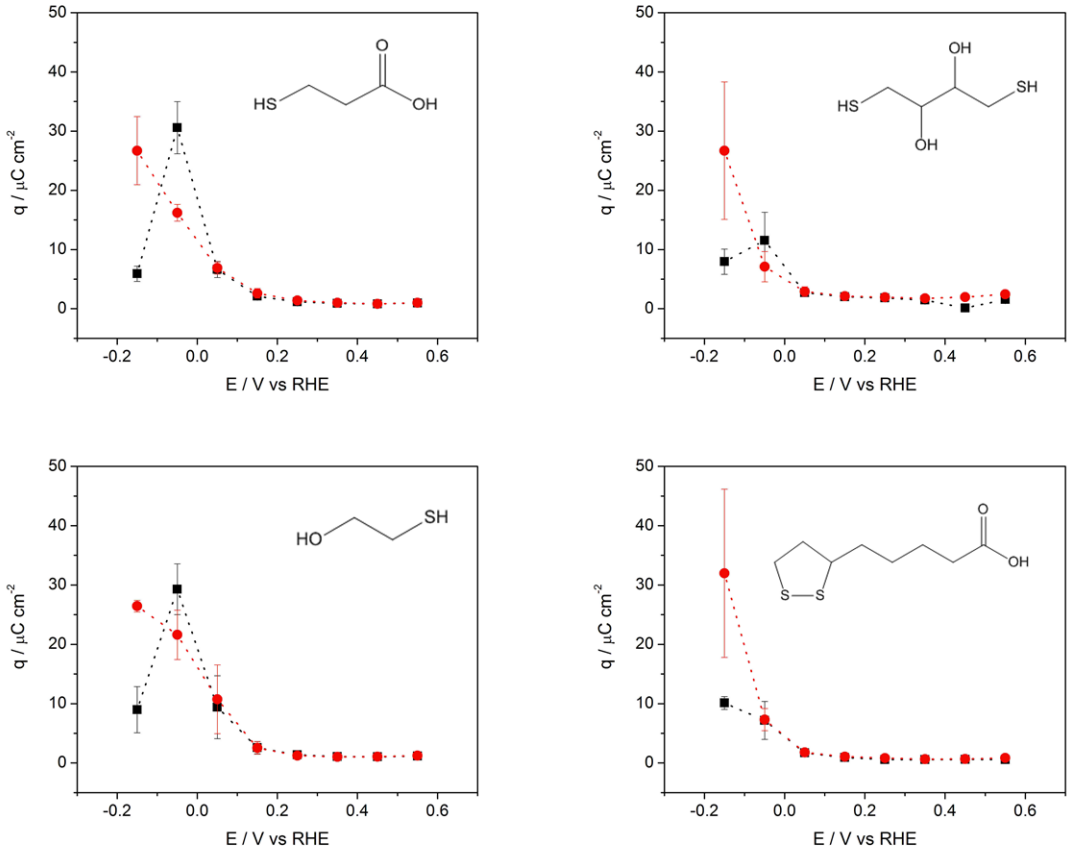

Figure 3. Charge of the reductive desorption from polycrystalline gold electrodes of the sulfur-containing compounds 1-4 obtained from step-potential chronoamperometries recorded with 1 s step at-0-05 (■) and -0.15 (●) V vs RHE.

Using the step-potential chronoamperometries we have determine the charge density curves for the thiol covered and thiol free electrodes in NaF and DPBS (figure S5). The charge corresponding to adsorbed thiol was determined by the difference between the charge measured for a thiol covered electrode and the charge measured in the nonadsorbing electrolyte (NaF).

The total charge of desorption of monothiols (**1**) and (**2**) were 66 ± 11 μC/cm^2 and 57 ± 10 μC/cm^2 respectively. Unfortunately due to the overlapping of the desorption of (**3**) and (**4**) with the hydrogen evolution reaction, it was not possible to determine the total charge of desorption of these molecules. the charge for the desorption of (**3**) and (**4**) in the potential region under study were 47± 16 μC/cm^2 and 45 ± 15 μC/cm^2 respectively.

Since the utilization of the sulfur-containing self-assembled monolayers in electrochemical sensors requires long term stability, we increased the duration of the probed potentials to 1 min. When the step potential was increased from 1s (Figure 3) to 1min (Figure S6) the desorption kinetics were identical. These results shows that the thiol desorption at a given potential is completed after 1s.

3.2 Effect of the surface structure on the stability of the SAMs: 3-mercaptopropionic acid vs DL-thioctic acid

As mentioned above, one of the parameters that governs the adsorption/desorption of these molecules from the gold surface is the surface structure. To investigate the surface structure dependent stability, layers of 3-mercaptopropionic acid (**1**) and DL-thioctic acid (**4**) adsorbed onto Au(100) and Au(111) electrodes in phosphate buffer saline solution were prepared, and their stability against the applied potential evaluated using cyclic voltammetry as described before. Anionic compounds (**1**) and (**4**) were selected because of the similarities in their chemical functionality, but presented significant differences in their stability on the polycrystalline gold surface (Fig. 1 and 3)

Fig. 4 shows voltammetric profiles of the Au(100) and Au(111) surface modified electrodes with 3-mercaptopropionic acid. Blank voltammetry of the bare gold electrodes in DPBS are included to demonstrate the quality of the single-crystal electrodes and the cleanness of the electrochemical cell and electrolyte. The voltammetry of the surfaces modified single-crystal electrodes showed a suppression of the features present on the blank voltammetry between 0.2 and 1 V which are

associated to the lifting of the reconstruction and the adsorption/desorption of the anions.[44] This confirms the presence of (**1)** adsorbed onto the surface of single crystal electrodes. In the negative scan, at potentials lower than 0.2 V, the voltammetric profiles of the modified electrodes displayed the reductive peak corresponding to desorption of 3-mercaptopropionic acid. When both single crystals were compared (Fig. 4C) it could be noticed that desorption of 3-mercaptopropionic acid from (111) sites was favoured. While the onset potential of the desorption of 3-mercaptopropionic acid on both electrodes takes place at similar potentials, desorption of (**1)** on the Au(111) takes place in a narrow potential window (0.2 and 0.05 V), while the desorption of 3-mercaptopropionic acid on Au (100) electrodes occurred over a broader potential window. These differences in the desorption potential (E_{des}) of thiols have been associated to a combination of the potential of zero charge (pzc) - provided for no specific adsorption of ions- and the strength of the intermolecular interaction -which it will depends on the number of Au-S bonds.[48]

The potential of zero charge is a fundamental property of the interface and its understanding is critical for a detailed description of the double layer phenomenon. However, the adsorption of thiols on the electrode surface may lead to a large shift of the potential of zero charge. When the electrode is covered by a thiol monolayer, the charge density (σ_M) of the Au electrode is a function of the electrode potential (E) and the surface Gibbs excess (Γ) of the monolayer. The charge measured during the reductive desorption process is called the total charge and includes both the charge flowing from the electrode to change the oxidation state of thiol molecules and the charging of the electrical double layer. The potential at which the total charge is equal to zero is referred as potential of the zero total charge (pztc) and depends on the number of Au-S bonds formed and the adsorption/desorption of anions[49, 50].

It is also important to notice that the coverage and packing of these compounds on the (111) and (100) crystal structure may differ. As was mentioned before, the desorption of thiols from gold surfaces is delayed to more negative potentials on closely packed self-assembled monolayers, which may justify the significantly larger value of charge ($85.3\pm 5.2\mu C\ cm^{-2}$) associated to the desorption

of 3-mercaptopropionic acid from the Au(111) electrode in comparison with the desorption from the Au(100) electrode (70.7±5.1 μC cm^{-2}).

It has been reported that the SAMs of 3-mercaptopropionic acid (**1**) on Au(111) surfaces in a pH 7 phosphate buffer pack into several phases.[51] The most predominant phase is an incommensurate p×√3 structure, but several commensurate (px√3) phases are also present. Due to the different phases of the thiols and inconmesurable nature of the structures it is not possible to accurately determine the number of molecules in the surface and thus the maximum coverage of 3-mercaptopropionic acid on the Au(111) electrode. No information has been previously reported on the adsorption of this compound on Au(100) surfaces, however the higher stability observed for its absorption on the Au(100) electrode might be associated to the conformation and packing of the 3-mercaptopropionic acid molecules on the Au(100) surface.

In the reverse scan, a broad peak between -0.15 V and 0.4 V vs RHE was observed, that was associated to the re-adsorption of desorbed molecules from the electrolyte. Such process is also remarkably kinetically-favoured by the presence of (111) sites giving a defined peak when compared to broad voltametric signal of re-adsorption on Au(100). The integrated charge for this process indicated that over 60 % of the desorbed molecules are re-adsorbed on both (111) and (100) sites.

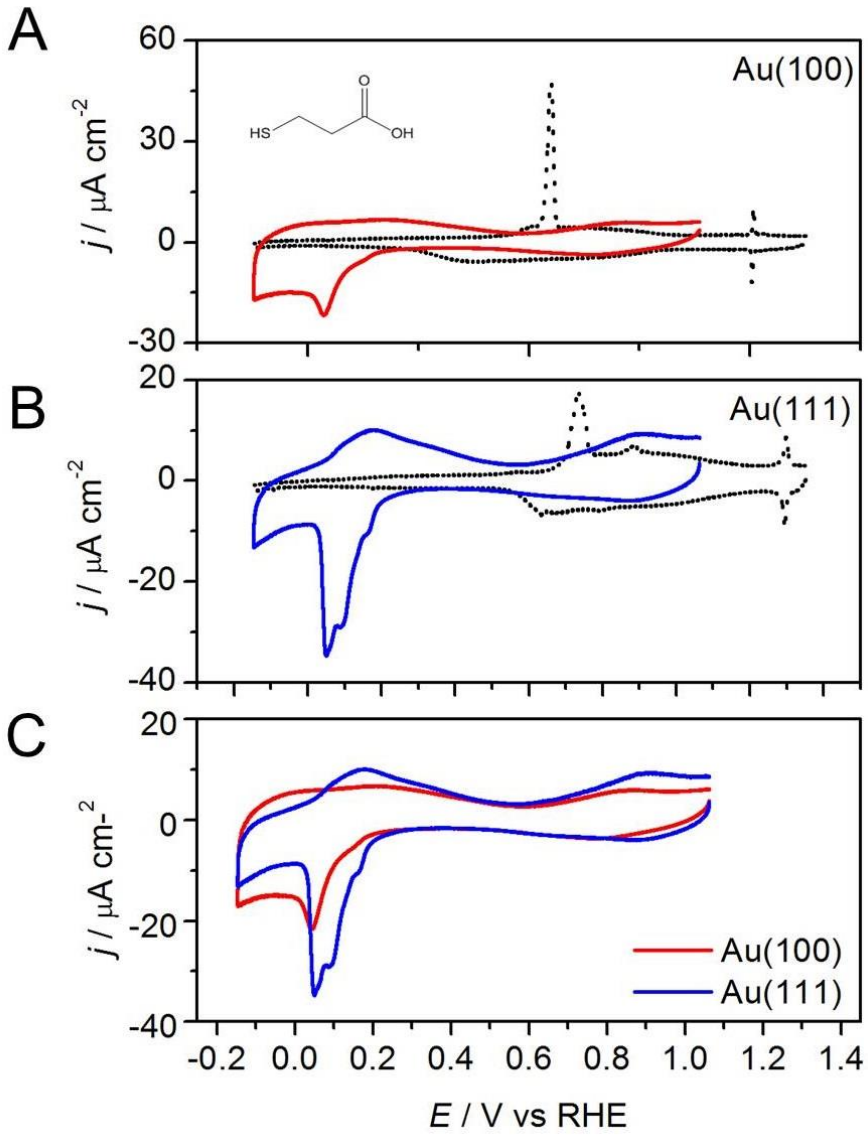

Figure 4. Voltammetric profiles of (A) Au(100), and (B) Au(111) modified with 3-mercaptopropionic acid (1) recorded in DPBS. Voltammetries of the single-crystal electrodes in absence of the adsorbed 3-mercaptopropionic acid are shown for comparison (dotted line). C) Comparison of Au(100) and Au(111) single crystal electrodes modified with (1). Scan rate υ = 50 mV s^{-1}.

Similar to the results presented above for (**1**), the voltametric profiles of the Au(100) and Au(111) electrodes modified with DL-thioctic acid (**4**) showed a suppression of the features associated to the adsorption of anions onto the gold electrode in the region between 1 and 0 V followed by the reductive desorption of the compound at potentials lower than 0 V (Figure 5). This potential was ~0.2 V lower than the desorption potential of 2-mercaptopropanoic acid (**1**), a clear indication of the

higher stability of the DL-thioctic acid (**4**) monolayers in comparison with those made with **1**, as shown previously for the polycrystalline electrode (Fig. 1 and 3). Moreover, the comparison between the reductive desorption of DL-thioctic acid (**4**) between both basal planes (Fig. 5C), clear indicates a higher stability of the DL-thioctic acid on the Au(100) electrode. While a rapid desorption takes place on the Au(111) electrode between 0 and -0.15 V, just a small fraction of compound (**4**) is desorbed from the Au(100) electrode in the same potential window. The desorption of DL-thiotic acid (**4**) from this electrode takes place at more negative potentials (Fig. S7) where the hydrogen evolution reaction (HER) on gold also takes place. This overlap prevents quantification of the charge associated to the desorption of the this disulphide from Au(100) surfaces. To our knowledge, this is the first time the stability of DL-thioctic acid (**4**) monolayers on single crystal gold electrodes has been evaluated.

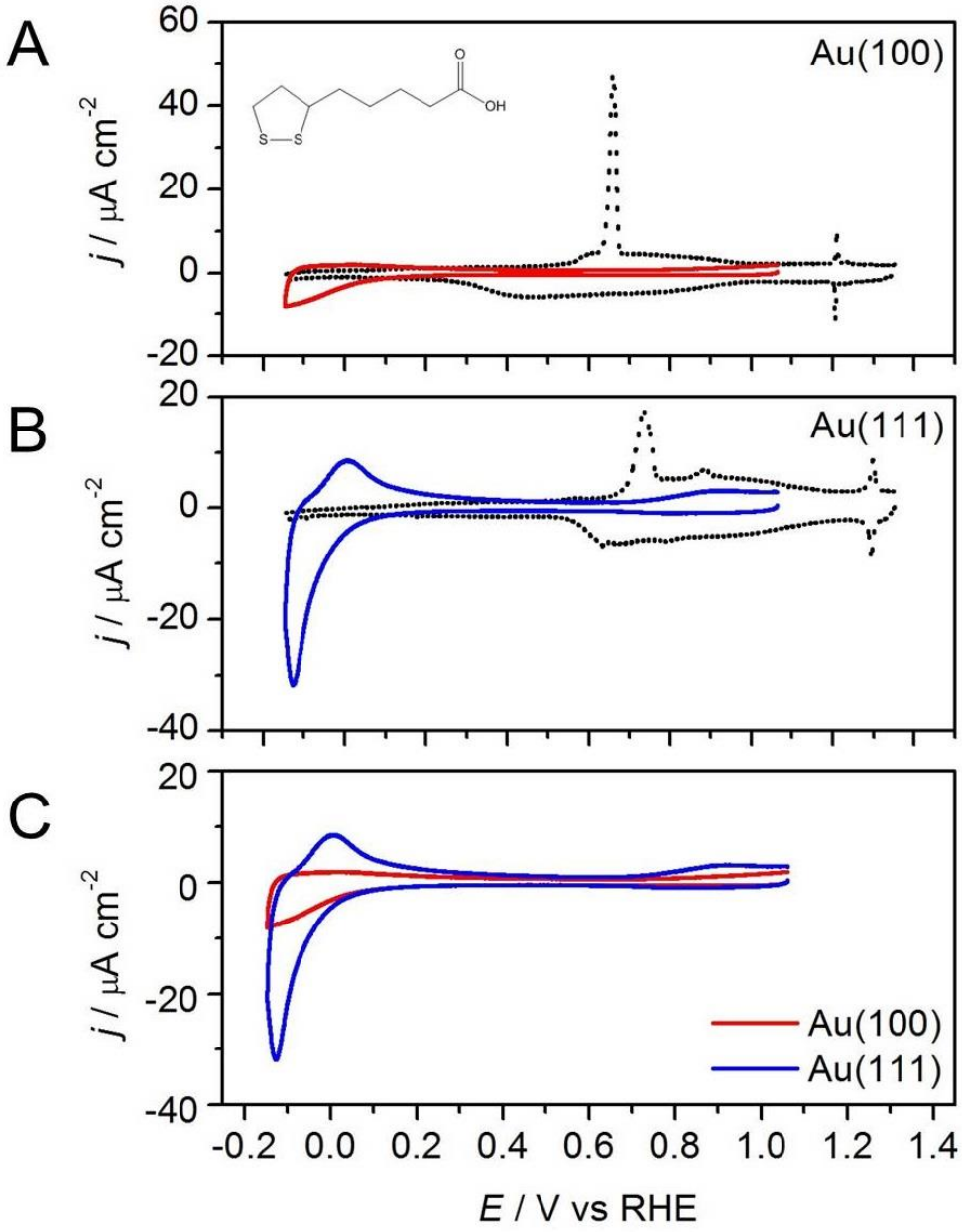

Figure 5: Voltammetric profiles of (A) Au(100), and (B) Au(111) modified with DL-thioctic acid (4) in DPBS solution. Voltammetries of the single-crystal electrodes in absence of the adsorbed 1 are shown for comparison (dotted line). C) Comparison of Au(100) and Au(111) single crystal electrodes modified with (4). Scan rate υ = 50 mVs^{-1}.

The superior stability of these compounds on the Au(100) electrode with respect to the Au(111) is in agreement with previous results for other thiols,[18] and has been attributed to the potential of zero charge. However when comparing the adsorption of monothiols vs disulfides, due to the difference in electron transfer, 1 vs 2 electron, one must consider the potential of zero total charge (pztc) instead of the potential of zero charge (pzc). Previous reports have shown significant differences

between numerical values of pzc and pztc of SAM on Au(111) electrodes.[15] Unfortunately, common strategies to determine the pztc such as charge displacement using carbon monoxide[52, 53] cannot be apply to determine the pztc of the SAMs of thiols and disulfides.

4. Conclusions

This manuscript provides important information regarding the parameters governing the stability of self-assembled monolayers of sulfur-containing molecules on Au electrodes in physiological media. In particular, we have implemented cyclic voltammetry and progressive step potential chronoamperometry to determine the stability of four representative sulfur-containing compounds, 3-mercaptopropionic acid (**1**), 2-mercaptoethanol (**2**), 1,4-dithiothreitol (**3**) and DL-thioctic acid (**4**), in physiological media as a function of the potential and the surface structure. The differences in desorption potential between these molecules can be attributed to the adsorption energy of the S-single and S-double coordination to the surface, to the strength of the lateral intermolecular interaction (resulting in different packing and coverage) and to the changes of the potential of zero total charge (pztc) of the surface.

Our results also show that the desorption of self-assembled monolayers of monothiols (**1**) and (**2**) on polycrystalline gold takes place at approximately 0.15 V vs RHE. In addition, we show that compounds (**3**) and (**4**), that carry two coordinating sulfur atoms in their structure, have an improved stability so that more negative potentials are required for the reductive desorption. Among these two, electrodes modified with DL-thioctic acid showed the highest potential-dependent and time-dependent stability, presumably due to stabilization through Van der Waals lateral interactions between hydrophobic aliphatic chains.[27] The possible application of Anson's monolayer model[54-56], as suggested by one reviewer of this manuscript, is limited in this case due to the complexity of the surface structure and adsorption sites on polycrystalline electrodes, the specific adsorption and replacement by anions during the thiol and disulphide desorption, and the overlapping of the hydrogen evolution signal with the desorption for 1,4-dithiothreitol (3) and DL-

thioctic acid (4). Finally, we report for the first time a higher stability on (100) sites when compared to (111) sites, for SAMs of compounds (**1**) and (**4**).

We believe our results contribute to the development and understating of more robust electrochemical systems such as electrochemical sensors. In addition, the reported methodology can be implemented for the study of the desorption kinetics of self-assembly monolayers relevant in the development of drug-released devices using electrochemical control.

Acknowledgements

AK acknowledges the University of Birmingham for the financial support through a PhD scholarship at the School of Chemistry. PR and FFT would like to acknowledge the University of Birmingham for the financial support through the Birmingham fellowship program. FFT also thanks John Evans (John Evans Fellowship) for the financial support.

References

1. X. Jiang, R. Ferrigno, M. Mrksich and G. M. Whitesides, *J. Am. Chem. Soc.*, 2003, **125**, 2366-2367.
2. R. S. Kane, S. Takayama, E. Ostuni, D. E. Ingber and G. M. Whitesides, *Biomaterials*, 1999, **20**, 2363-2376.
3. T. Wink, S. J. van Zuilen, A. Bult and W. P. van Bennekom, *Analyst*, 1997, **122**, 43R-50R.
4. J. C. Love, L. A. Estroff, J. K. Kriebel, R. G. Nuzzo and G. M. Whitesides, *Chem. Rev.*, 2005, **105**, 1103-1170.
5. C. Vericat, M. E. Vela, G. Benitez, P. Carro and R. C. Salvarezza, *Chem. Soc. Rev.*, 2010, **39**, 1805-1834.
6. F. P. Zamborini and R. M. Crooks, *Langmuir*, 1998, **14**, 3279-3286.
7. P. E. Laibinis and G. M. Whitesides, *J. Am. Chem. Soc.*, 1992, **114**, 9022-9028.
8. D. Pissuwan, T. Niidome and M. B. Cortie, *J. Controlled Release*, 2011, **149**, 65-71.
9. J. Gao, X. Huang, H. Liu, F. Zan and J. Ren, *Langmuir*, 2012, **28**, 4464-4471.
10. C. D. Hodneland and M. Mrksich, *Langmuir*, 1997, **13**, 6001-6003.
11. S. S. Agasti, A. Chompoosor, C.-C. You, P. Ghosh, C. K. Kim and V. M. Rotello, *J. Am. Chem. Soc.*, 2009, **131**, 5728-5729.
12. C. D. Hodneland and M. Mrksich, *J. Am. Chem. Soc.*, 2000, **122**, 4235-4236.
13. J. Kunze, J. Leitch, A. L. Schwan, R. J. Faragher, R. Naumann, S. Schiller, W. Knoll, J. R. Dutcher and J. Lipkowski, *Langmuir*, 2006, **22**, 5509-5519.
14. T. Laredo, J. Leitch, M. Chen, I. J. Burgess, J. R. Dutcher and J. Lipkowski, *Langmuir*, 2007, **23**, 6205-6211.
15. Z. Su, J. Leitch and J. Lipkowski, *Zeitschrift für Physikalische Chemie International journal of research in physical chemistry and chemical physics*, 2012, **226**, 995-1009.
16. E. Chow, D. B. Hibbert and J. J. Gooding, *Anal. Chim. Acta*, 2005, **543**, 167-176.
17. E. Chow, D. B. Hibbert and J. J. Gooding, *Analyst*, 2005, **130**, 831-837.

18. Z. L. Yu, J. Casanova-Moreno, I. Guryanov, F. Maran and D. Bizzotto, *J. Am. Chem. Soc.*, 2015, **137**, 276-288.
19. C.-J. Zhong, J. Zak and M. D. Porter, *J. Electroanal. Chem.*, 1997, **421**, 9-13.
20. M. M. Walczak, D. D. Popenoe, R. S. Deinhammer, B. D. Lamp, C. Chung and M. D. Porter, *Langmuir*, 1991, **7**, 2687-2693.
21. D. F. Yang, C. P. Wilde and M. Morin, *Langmuir*, 1996, **12**, 6570-6577.
22. M. M. Walczak, C. A. Alves, B. D. Lamp and M. D. Porter, *J. Electroanal. Chem.*, 1995, **396**, 103-114.
23. F. Loglio, M. Schweizer and D. M. Kolb, *Langmuir*, 2003, **19**, 830-834.
24. N. S. Pesika, K. J. Stebe and P. C. Searson, *Langmuir*, 2006, **22**, 3474-3476.
25. D. F. Yang and M. Morin, *J. Electroanal. Chem.*, 1998, **441**, 173-181.
26. W. H. Mulder, J. J. Calvente and R. Andreu, *Langmuir*, 2001, **17**, 3273-3280.
27. M. D. Porter, T. B. Bright, D. L. Allara and C. E. D. Chidsey, *J. Am. Chem. Soc.*, 1987, **109**, 3559-3568.
28. S.-S. Wong and M. D. Porter, *J. Electroanal. Chem.*, 2000, **485**, 135-143.
29. J. D. C. Jacob, T. R. Lee and S. Baldelli, *J. Phys. Chem. C*, 2014, **118**, 29126-29134.
30. D. F. Yang, H. Al-Maznai and M. Morin, *J. Phys. Chem. B*, 1997, **101**, 1158-1166.
31. J. L. Shepherd, A. Kell, E. Chung, C. W. Sinclar, M. S. Workentin and D. Bizzotto, *J. Am. Chem. Soc.*, 2004, **126**, 8329-8335.
32. B. Cui, T. Chen, D. Wang and L.-J. Wan, *Langmuir*, 2011, **27**, 7614-7619.
33. E. Pensa, C. Vericat, D. Grumelli, R. C. Salvarezza, S. H. Park, G. S. Longo, I. Szleifer and L. P. M. De Leo, *Physical Chemistry Chemical Physics*, 2012, **14**, 12355-12367.
34. M. J. Esplandiu, M. L. Carot, F. P. Cometto, V. A. Macagno and E. M. Patrito, *Surface Science*, 2006, **600**, 155-172.
35. P. Mali, N. Bhattacharjee and P. C. Searson, *Nano Lett.*, 2006, **6**, 1250-1253.
36. D. Svirskis, J. Travas-Sejdic, A. Rodgers and S. Garg, *J. Controlled Release*, 2010, **146**, 6-15.
37. M. B. Fritzen-Garcia, V. C. Zoldan, I. R. W. Z. Oliveira, V. Soldi, A. A. Pasa and T. B. Creczynski-Pasa, *Biotechnol. Bioeng.*, 2013, **110**, 374-382.
38. A. Cossaro, R. Mazzarello, R. Rousseau, L. Casalis, A. Verdini, A. Kohlmeyer, L. Floreano, S. Scandolo, A. Morgante, M. L. Klein and G. Scoles, *Science*, 2008, **321**, 943-946.
39. M. Byloos, H. Al-Maznai and M. Morin, *J. Phys. Chem. B*, 1999, **103**, 6554-6561.
40. N. C. III, C. E. D. Chidsey, G. y. Liu and G. Scoles, *J. Chem. Phys.*, 1993, **98**, 4234-4245.
41. J. Souza-Garcia, A. Berná, E. A. Ticianelli, V. Climent and J. M. Feliu, *J. Electroanal. Chem.*, 2011, **660**, 276-284.
42. J. Cui, Y. Yan, Y. Wang and F. Caruso, *Adv. Funct. Mater.*, 2012, **22**, 4718-4723.
43. Y. A. Romanov, A. N. Darevskaya, N. V. Merzlikina and L. B. Buravkova, *Bulletin of Experimental Biology and Medicine*, 2005, **140**, 138-143.
44. A. Cuesta, M. Kleinert and D. M. Kolb, *Phys. Chem. Chem. Phys.*, 2000, **2**, 5684-5690.
45. E. Pensa, C. Vericat, D. Grumelli, R. C. Salvarezza, S. H. Park, G. S. Longo, I. Szleifer and L. P. Mendez De Leo, *Phys. Chem. Chem. Phys.*, 2012, **14**, 12355-12367.
46. C. A. Widrig, C. Chung and M. D. Porter, *J. Electroanal. Chem.*, 1991, **310**, 335-359.
47. L. Y. S. Lee and R. B. Lennox, *Langmuir*, 2007, **23**, 292-296.
48. T. Doneux, M. Steichen, A. De Rache and C. Buess-Herman, *J. Electroanal. Chem.*, 2010, **649**, 164-170.
49. W. Schmickler and E. Santos, *Interfacial electrochemistry*, Springer Science & Business Media, 2010.
50. V. Climent, R. Gomez, J. Orts, A. Aldaz and J. Feliu, *Electrochemical Double Layer*, 1997, **97**, 17.
51. M. J. Giz, B. Duong and N. J. Tao, *J. Electroanal. Chem.*, 1999, **465**, 72-79.
52. J. Clavilier, R. Albalat, R. Gomez, J. M. Orts, J. M. Feliu and A. Aldaz, *J. Electroanal. Chem.*, 1992, **330**, 489-497.
53. B. Alvarez, V. Climent, A. Rodes and J. M. Feliu, *Phys. Chem. Chem. Phys.*, 2001, **3**, 3269-3276.
54. Y. Xie and F. C. Anson, *Journal of Electroanalytical Chemistry*, 1995, **384**, 145-153.
55. Y. Xie and F. C. Anson, *Journal of Electroanalytical Chemistry*, 1995, **396**, 441-449.
56. Y. Xie and F. C. Anson, *Journal of Electroanalytical Chemistry*, 1996, **404**, 209-213.